

Laboratory Testing on Hydraulic Fracturing of Barre Granite:

Studying Visual Observations, Acoustic Emissions and Radiated Energy Related to Fracture Mechanisms

Auteur(e)s : Michela Casanova

Encadrement : Prof. Lyesse Laloui¹ / Prof. Herbert H. Einstein²

¹ Soil Mechanics Laboratory (LMS) EPFL / ² MIT CEE Rock Mechanics Group, MIT

Abstract Hydraulic fracturing is frequently used to increase the permeability of rock formations. This can be done by creating new fractures as usually done for hydrocarbon extraction or extending and opening fractures as usually done in Enhanced Geothermal Systems (EGS). In both cases, only indirect information such as in-situ stress, pumping records and microseisms are recorded. However, understanding the exact processes of hydraulic stimulation remains very challenging as some of the fundamental aspects such as the fracturing processes and induced/triggered seismicity are still unknown. Unique equipment developed by the MIT CEE Rock Mechanics Group allows one to visually observe hydraulic fracturing while recording Acoustic Emissions (AE) simultaneously. Important information is obtained by applying different fluid pressure in individual pre-cut flaws with distinct flow rates and external stresses. This research focuses on the main processes inducing hydraulic fracturing, and particularly hydro-shearing, by relating the AE data to visual observations, and investigating different experimental concepts in terms of focal mechanisms and normalized radiated seismic energy. In this work we show that (1) hydro-shearing may be induced by applying high external loads i.e. induce global shear failure; (2) local failure around the flaw tips is expected to occur in tensile mode; (3) the AE hypocenter location matches well with the visual crack observations; (4) some differences of focal mechanisms based on AE data and visual observations exist; (5) cyclic pressurization results in high normalized radiated seismic energy.

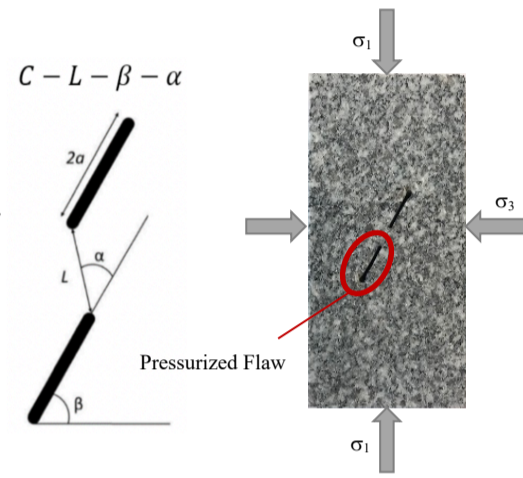
1. Background

1.1. Barre Granite Specimens

Size: 2"x 4"x 1" (101.6[mm] x 50.08[mm] x 25.4[mm])

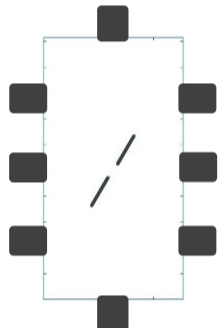
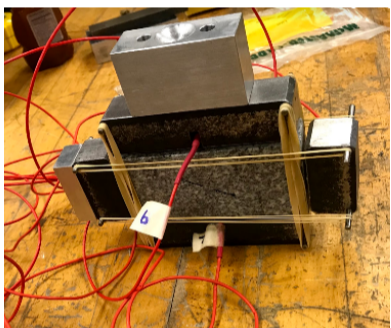
Notation of the double-flaw geometry developed by the MIT CEE Rock Mechanics Group:

- C: Material composition
- L: Ligament length (space between inner flaw tips)
- β: Flaw inclination with respect to the horizontal
- α: bridging angle



1.2. Acoustic Emissions

When recording AE data during the experiments, the AT data handling can be done using the MATLAB code developed by Li, (2019) allowing one to interpret the following information:



- Hypocenter locations
- Focal mechanisms
- Moment magnitude of the events
- Time of occurrence of the events

2. Experimental Setup, Devices & Concepts

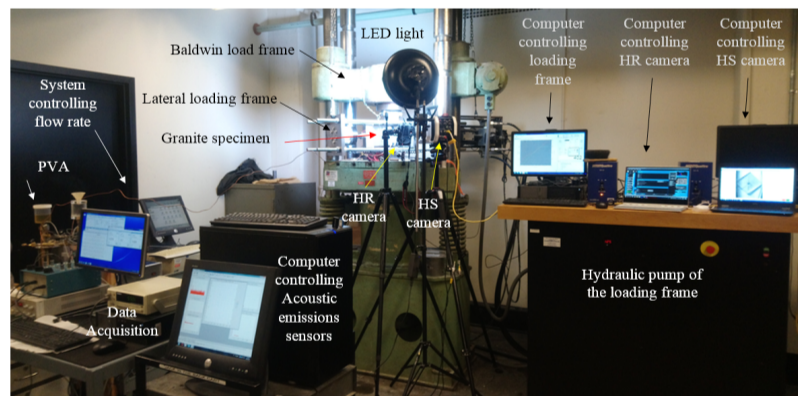
2.1. Overall Setup

High-Speed (HS) Camera:

- Up to 10'000 frames per second

High-Resolution (HR) Camera:

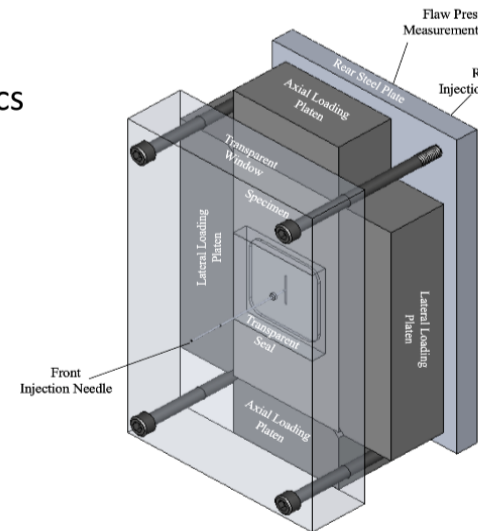
- Up to 20 mega pixels per image



2.2. Single Flaw Pressurization Device

Unique equipment developed by the MIT CEE Rock Mechanics Group allowing one to:

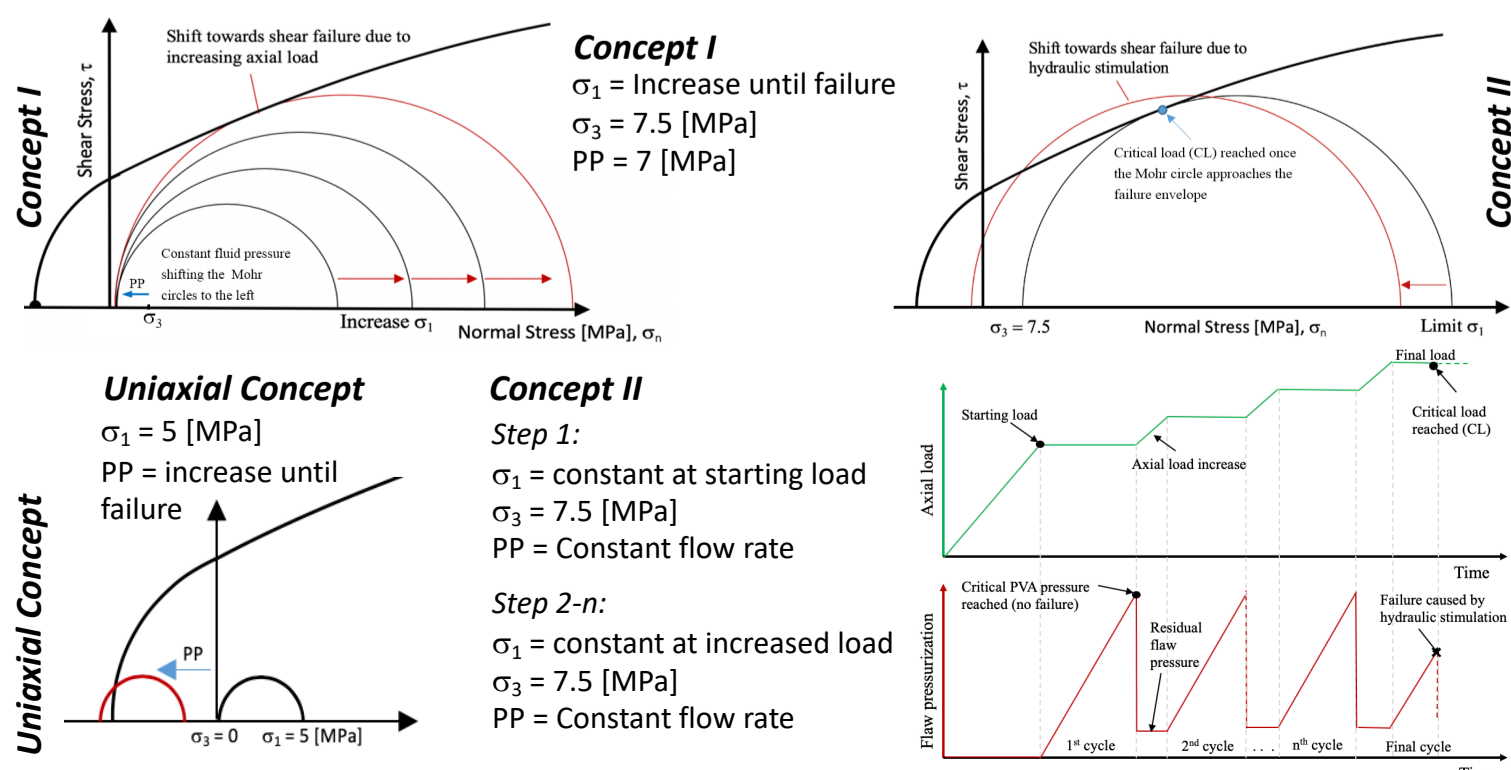
- Hydraulically pressurize one flaw
- Apply uniaxial/biaxial load
- Conduct visual observations of the front face of the specimen
- Record acoustic emissions



2.3. Research Questions Addressed in this thesis

- 1) Which are the main parameters (loading scenarios, flaw pair geometry) that induce hydro-shearing for this type of laboratory studies?
- 2) How do AE relate to visual observations in laboratory studies?
- 3) What are the relationships between the different experimental in terms of focal mechanisms and normalized radiated seismic energy?

2.4. Experimental Concepts

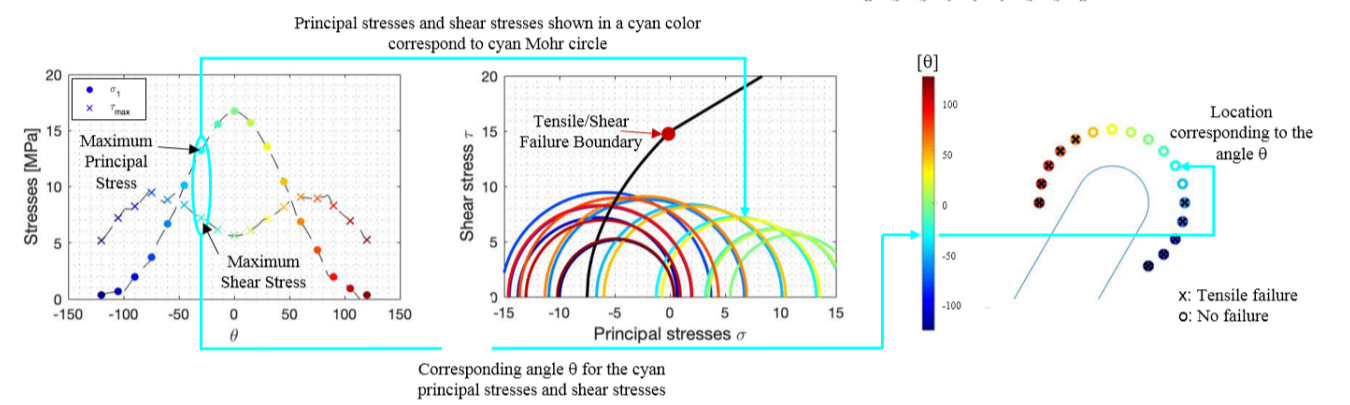


3. Numerical Study using MATLAB PDE Toolbox & Mohr-Coulomb Failure Criterion

Structural, linear elastic, static-plane-stress-analysis

Model allowing one to apply:

- Different loading conditions (biaxial/uniaxial and pressure in the flaw/s)
- Analyze different flaw pair geometries



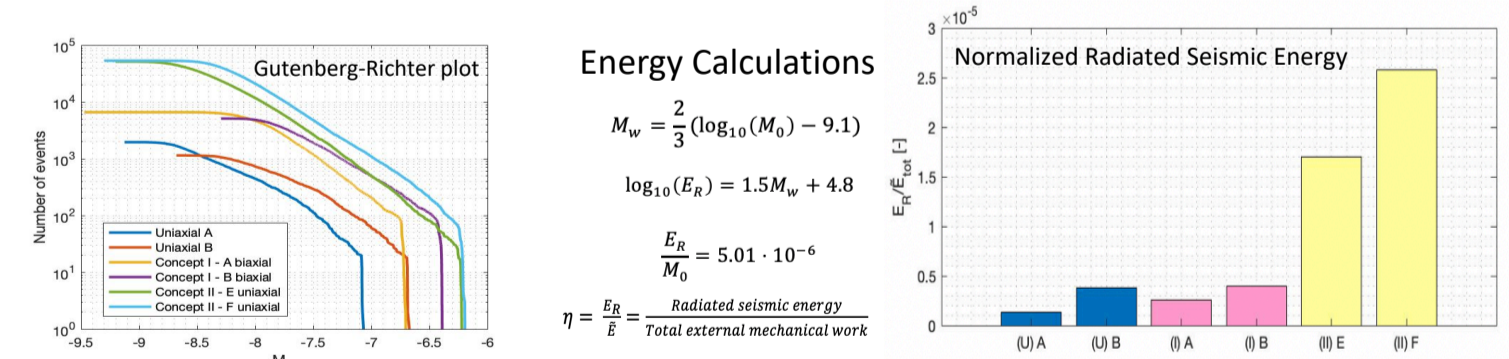
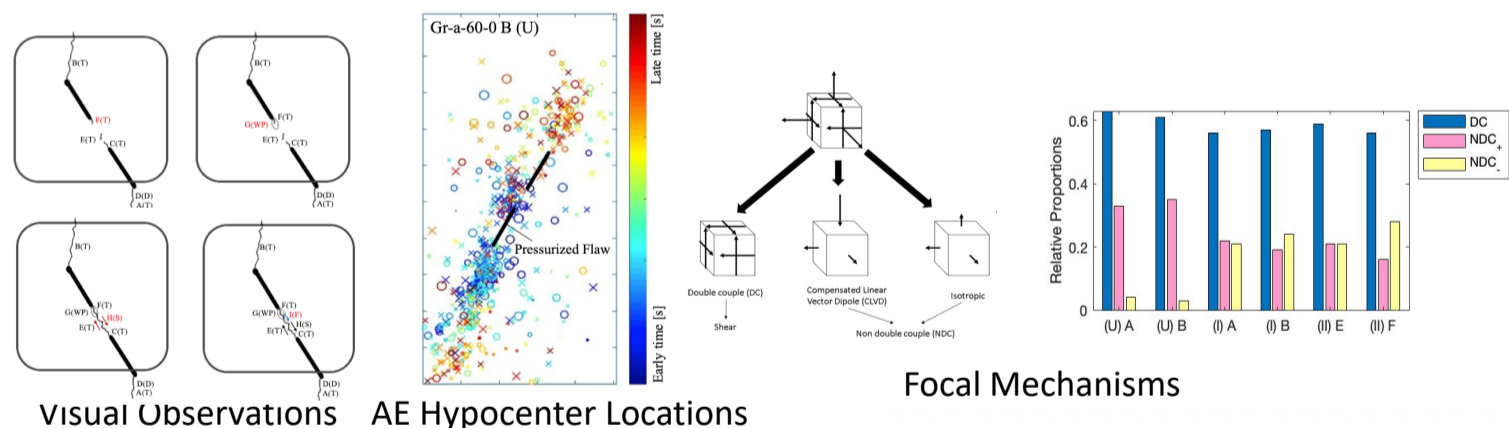
4. Experimental Results

4.1. Overview of the Experiments

Experiment	Concept	σ_{max} [Mpa]	σ_3 [Mpa]	Loading	# Pressurization cycles	P_{max} [Mpa]
Gr-a-60-0 A (U) ^a	Uniaxial	5	[-]	Uniaxial	1	9.5
Gr-a-60-0 B (U) ^a	Uniaxial	5	[-]	Uniaxial	1	9.7
Gr-a-60-0 (I) A ^a	I	81.2	7.5	Biaxial	est.	7
Gr-a-60-0 (I) B ^a	I	137	7.5	Biaxial	est.	7
Gr-a-60-0 (I) Dry ^a	I	142.4	7.5	Biaxial	[-]	[-]
Gr-a-60-0 (I) R	I	113.6	7.5	Biaxial	est.	7
Gr-a-15-0 (II) A	II	100	7.5	Biaxial	5	13.6 ^b
Gr-a-15-0 (II) B	II	110	7.5	Biaxial	8	13.6 ^b
Gr-a-60-0 (II) A	II	80	7.5	Biaxial	2	13.6 ^b
Gr-a-60-0 (II) B	II	129.2	9.5	Biaxial	13	13.6 ^b
Gr-a-60-0 (II) C	II	115	7.5	Biaxial	7	13.6 ^b
Gr-a-60-0 (II) D	II	112.2	7.5	Biaxial	3	13.6 ^b
Gr-a-60-0 (II) E	II	51.4	[-]	Uniaxial	2	8.5 ^b
Gr-a-60-0 (II) F	II	65	[-]	Uniaxial	4	5.55

^a Experiments conducted by de Saussure, (2018)
^b Maximum pump capacity reached

4.2. Visual Observations, Acoustic Emission Analysis and Energy Calculations



5. Conclusions & Further Research

- Hypocenter location analysis shows that AE events are well aligned with the visual observations
- Visual observations of focal mechanisms are not entirely in agreement with focal mechanisms observed in the AE analysis
- Difference in normalized radiated seismic energy for different experimental concepts
- Cyclic pressurization could have an effect on the normalized radiated seismic energy and may thus cause larger seismic damage for similar external mechanical work done

Further Research: Conduct further cyclic pressurization experiments, notably biaxial experiments and compare the energy calculations to the uniaxial experiments → draw further conclusions concerning the effect of cyclic pressurization

